International Conference on Applied Energy 2019
Aug 12-15, 2019, Västerås, Sweden
Paper ID: 1056

TEMPORAL AND SPATIAL ANALYSIS ON TEMPERATURES IN A SOFC SHORT STACK

Hangyue Li[1], Minfang Han[1,*], Qingping Fang[2], Zaihong Sun[3]

1 State Key Laboratory of Power Systems, Department of Energy and Power Engineering, Tsinghua University, Beijing, 100084, P.R. China

2 Institute of Energy and Climate Research (IEK), IEK-3, Forschungszentrum Jülich GmbH, 52425, Germany

3 Suzhou Huatsing Power Co., Ltd, Jiangsu, 210094, P.R. China

ABSTRACT

The distributions and transients of temperature are practical indicators of the state and the properties of Solid Oxide Fuel Cells (SOFCs), yet few methods are available to interpret the temperatures in-situ for the internal states of the stack. A heat balance model was developed to estimate the distribution of heat sources in a Solid Oxide Fuel Cell short stack. The model is based on the temperatures measured with 6 thermocouples in the stack and treats the stack as 6 elements, taking into account the heat transfer among the elements and the test bench. A significant change in heat source distribution before and after tests with carbon-containing gases was revealed with the model, indicating possible cell damage near the fuel inlet. The model will be further calibrated for better accuracy and spatial resolution.

Keywords: Solid Oxide Fuel Cell, Stack, Temperature, Heat Balance, Model, Heat Source

NONMENCLATURE

Abbreviations	
SOFC	Solid Oxide Fuel Cell
EIS	Electrochemical Impedance Spectroscopy

1. INTRODUCTION

SOFCs are devices that convert the chemical energy in fuels directly to electricity and heat. They have been widely studied since the past century. In experiments on SOFCs, cell voltages and temperatures are frequently measured and displayed in-situ. However, cell voltages and temperatures alone reveal little about the internal state and changes in a stack that may be closely relevant to the efficiency and rate of energy conversion. Many efforts have been made for an insight of the state and changes in working SOFCs. Some researchers measure the temperatures experimentally. Kirtley J. D. et al.[1] designed a special apparatus for in-situ optical monitoring and measured the steady temperature field and gas components at the anode surface simultaneously. Other researchers employ numerical simulation methods. Li A. et al.[2] developed and calibrated a 3D multi-physics CFD model and simulated steady states of a 30-layer stack that helped revealing the multi-physics coupling in such a large stack. Nishida, R. T. et al.[3] combined detailed temperature and voltage measurement and numerical simulation of a Mark-F stack from Jülich Research Center, Germany.

However, these studies require either specially designed experiment apparatus or elaborate modelling and calibration before any useful results are obtained. The optical measurements of Kirtley[1] require that the measured button cell exposes its electrode to the optical window, so that the infrared rays can reach out for spectroscopy or imaging, while the CFD models by Li A. et al.[2] and by Nishida, R. T. et al.[3] require the detailed geometries and material properties of the tested stack. These simulations are particularly informative when compared to the measured data, but are practically infeasible for in-situ interpretation of the measured data so far.

In this study, a data processing model for heat sources in the stack was developed. The intensity and distribution of the heat sources reveal how the electrochemical or chemical reactions distributed and evolved during the test. Intended for in-situ data analysis, the model is based on the simplified geometry of the stack and responds quickly to input data including measured temperatures and gas flow rates.

Selection and peer-review under responsibility of the scientific committee of the 11th Int. Conf. on Applied Energy (ICAE2019).

2. EXPERIMENTAL

2.1 Preparations

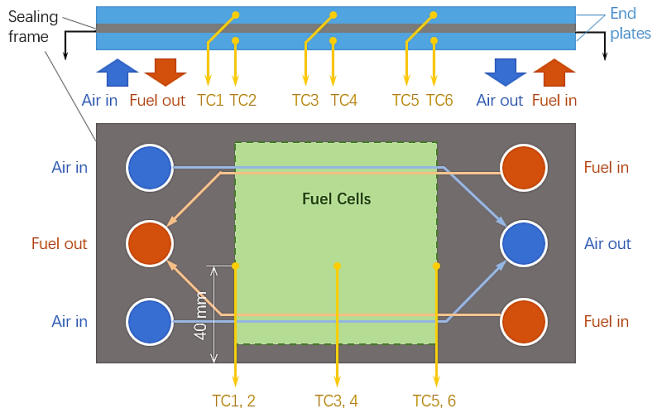

Fig 1 A schematic sketch of the stack configuration

A two-layer fuel cell stack was tested at Jülich Research Center, Germany. The stack comprises an F10 stack frame from Jülich Research Center and two 10 × 10 cm^2 anode supported planar SOFCs produced by Huatsing Power Co., Ltd. China. Each cell comprises a NiO-YSZ (8%mol Y_2O_3-stabilized ZrO_2) anode, an 8YSZ electrolyte, a GDC ($Gd_{0.1}Ce_{0.9}O_{2-\delta}$) barrier layer and a LSCF ($La_{0.6}Sr_{0.4}Co_{0.2}Fe_{0.8}O_{3-\delta}$) cathode. The active area of the anode or the cathode of each cell in the F10 stack was 80 cm^2. The stack was tested in a test bench with a 600 × 600 × 600 mm^3 electrically heated hood. The electrical current through the stack was tapped from the top and the bottom of the stack.

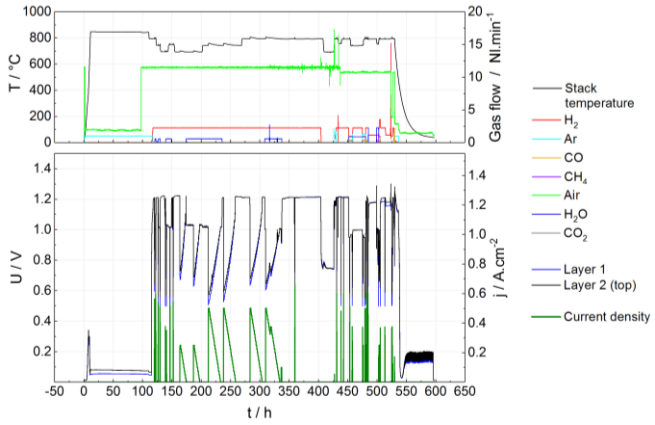

Fig 2 Time plot of the whole test

As is shown in Fig 1, gases for the anode and the cathode were fed and vented from the bottom of the stack. The stack was operated in counter flow configuration and the voltage of each cell was monitored throughout the test. There are three φ2 mm holes for thermocouples on each of the top and the bottom end-plate of the stack as is shown in Fig 1. The holes are 40 mm deep and are positioned above and under the active area of the cells near the fuel inlet, in the middle and near the fuel outlet. The above-mentioned temperatures, gas flow rates, voltages and etc. were sampled every user-specified time interval, which can be changed during the test.

2.2 Design of Experiment

The stack was sealed and the cells were reduced following the standard procedures in the research center. After the reduction, the stack was immediately tested at furnace temperature 800°C with dry hydrogen for EIS data and then a polarization curve as benchmark 1. The flow rate of hydrogen was 2.23 NL/min (liter gas per minute at standard conditions) so that the fuel utilization was 50% when the average current density per geometry electrolyte area per cell equals 1 A/cm^2. All benchmarks were recorded under identical furnace temperature, fuel composition, fuel flow rate and fuel preheater temperature. The air flow rate was changed from 12 NL/min to 10 NL/min due to problems of the air mass flow controller. Tests with hydrogen and carbon-containing gases were done after benchmark 1 and before benchmark 5. The furnace temperature, gas flow rates, electrical current and cell voltages throughout the whole test are illustrated in Fig 2. In the following sections, benchmark 1 in the 121th hour and benchmark 5 in the 514th hour are analyzed in detail. The other parts of the test will be analyzed in future studies.

3. RESULTS AND DISCUSSION

3.1 Theory & Calculation: The Heat Balance Model

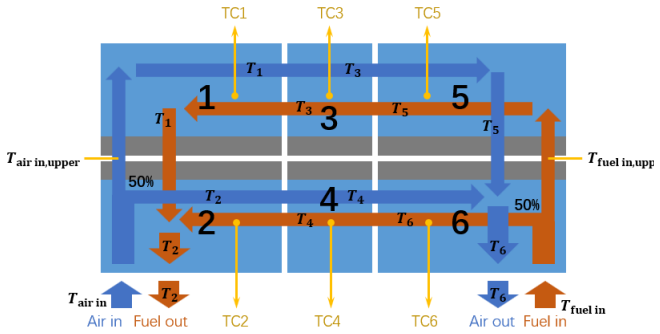

Fig 3 A schematic sketch of the simplified geometry of the stack

A heat balance model was developed based on the simplified geometry of the stack. As is shown in Fig 3, the stack is split into 6 elements. Each element is assumed to have a uniform temperature distribution and its temperature is given by the corresponding thermocouple. The inlet air and fuel temperatures are $T_{\text{air in}}$ and $T_{\text{fuel in}}$, respectively. 50% of the total air or

fuel flows into the upper layer and the other 50% flows to the lower layer. The gas composition entering each layer is assumed identical. The air and fuel leaving the lower layer and entering the upper layer are at $T_{\text{air in,upper}}$ and $T_{\text{fuel in,upper}}$, respectively. $T_{\text{air in,upper}}$ and $T_{\text{fuel in,upper}}$ can be different from T_2 and T_6 because the gases may not have reached thermal equilibrium with the solid walls before entering the upper layer.

$$m_{\text{elem}} c_{\text{p,s}} \frac{\partial T}{\partial t} = S - Q_{\text{out}} - \sum_{i}^{\text{gases}} \dot{N}_i c_{\text{p},i} \left(T_{i,\text{out}} - T_{i,\text{in}}\right) \quad [1]$$

The heat balance model takes into account the heat conduction in solid materials, the heat transfer between the elements and its surrounding and the gases inside the stack. For each element, the corresponding heat source is calculated with equation [1], where m_{elem} is the mass of the element, $c_{\text{p,s}}$ is the heat capacity of the element (equivalent solid heat capacity), $\frac{\partial T}{\partial t}$ is the derivative of temperature to time, S is the heat generation rate of the heat source in the element, Q_{out} is the heat flowing outward the element excluding the heat transfer with the gas flow inside the stack, the i in the summation denotes air or fuel in a certain flow path, "gases" means fuel and air in all flow paths, $\dot{N}_i$ is the mole flow rate of i, $c_{\text{p},i}$ is the heat capacity at constant pressure of i, $T_{i,\text{out}}$ and $T_{i,\text{in}}$ are the gas temperature leaving and entering the element of i, respectively.

Note that the heat source S involves the heat in electrochemical and catalyzed reactions, as well as the ohmic heat in the cells and stack components. During benchmark 1 and benchmark 5, the heat in catalyzed reactions was negligible compared to the heat in electrochemical reactions and the ohmic heat, because only hydrogen was used as the fuel.

3.2 Analysis on benchmark 1

During the polarization test of benchmark 1, the current kept increasing until the voltage of one of the two cells reached 0.6 V. Then the current started to decrease until it reached 0 A. The maximum current was 45 A, corresponding to an average current density of 0.56 A/cm^2 per active anode or cathode geometry area. During the polarization test, the temperature at position 3 increased by 8.8 °C and the maximum temperature difference among the 6 measured positions increased from 6.9 °C to 11.0 °C.

For comparison, the polarization losses of the lower and the upper cell is calculated with equation [2] and are plotted together in Fig 4 with the sums of the heat sources calculated with the heat balance model, see equations [3] and [4]. In equation [2], the i denotes the lower or upper cell, I denotes the stack current and $V_{\text{OC},i}$ denotes the open circuit voltage of cell i immediately before the polarization test. The subscript "total" means the sum of the values of the upper cell and the lower cell. Theoretically, for each cell the polarization loss equals the heat generation rate.

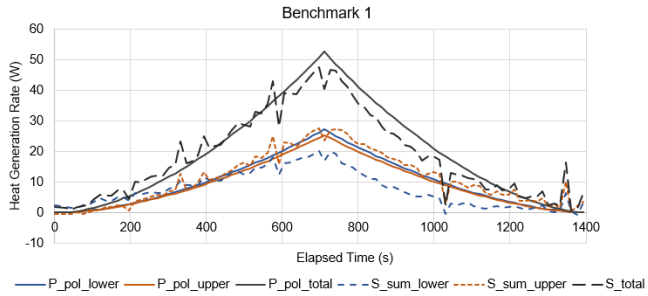

Fig 4 Comparison of the Polarization Loss and the Estimated Heat Sources

$$P_{\text{pol},i} = I \cdot \left(V_{\text{OC},i} - V_i\right) \quad [2]$$

$$S_{\text{sum,lower}} = S_2 + S_4 + S_6 \quad [3]$$

$$S_{\text{sum,upper}} = S_1 + S_3 + S_5 \quad [4]$$

As is shown in Fig 4, the estimated total heat generation rates of the heat sources agree well with the total polarization losses in benchmark 1. The relative error is 37% for the lower cell, 22% for the upper cell and 17% for the two cells as a whole. In the first 600 seconds, the relative error of the sum of all 6 heat sources is 12%. Therefore, heat sources 1 and 2, 3 and 4, 5 and 6 are treated together in the following analysis and the estimated heat sources in the first 600 seconds are believed to be more accurate.

Fig 5 shows the heat sources near the fuel outlet, in the middle and near the fuel inlet during the polarization

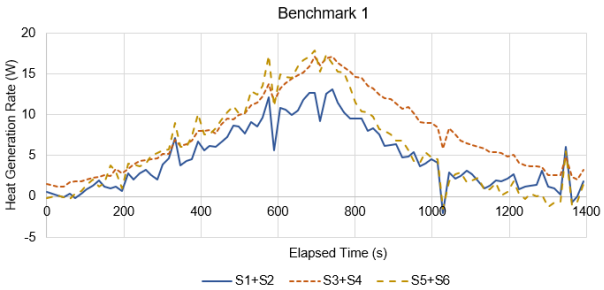

Fig 5 Estimated heat sources near the fuel outlet ($S_1 + S_2$), in the middle ($S_3 + S_4$) and near the fuel inlet ($S_5 + S_6$) in benchmark 1

test of benchmark 1. In the first 600 seconds, the average heat source near the fuel outlet was 30% lower than near the fuel inlet. Note that the fuel utilization was 23% calculated with the last data sample in the first 600 seconds of the polarization test with a current of 37 A, indicating that the distribution of the estimated heat source is reasonable.

3.3 Comparison of benchmarks 1 and 5

Benchmark 5 was recorded 393 hours after benchmark 1. Between the two benchmarks, tests with CO-containing gases and methane were done and a pronounced decrease of cell voltages under load was observed, indicating cell degradation or damage, as is shown in Fig 6.

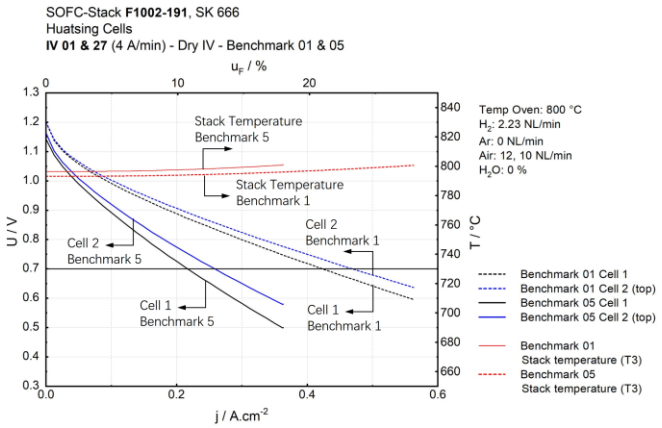

Fig 6 I-V curves in benchmark 1 and benchmark 5

The estimated heat sources reflect the degradation and provided spatial information regarding the degradation. As is shown in Fig 7, the heat sources near the fuel inlet ($S_5 + S_6$) were considerably weaker than those in the middle or near the fuel outlet.

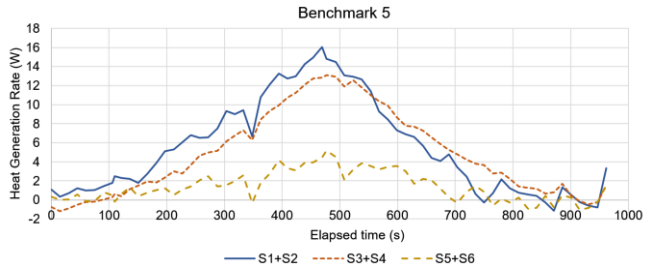

Fig 7 Estimated heat sources near the fuel outlet ($S_1 + S_2$), in the middle ($S_3 + S_4$) and near the fuel outlet ($S_5 + S_6$) in benchmark 5

After benchmark 5, the stack was further tested with hydrogen and CO-containing gases during a 6-hour period. Then the stack was cooled down and dissembled for post-mortem analysis. Fig 8 shows the anode of the upper cell after test. Above and under the 5 cm mark on the right side, the anode region near the fuel inlet is highly pulverized and appears lighter than near the fuel outlet below. Further analysis on the composition of the powder is required to reveal the occurring time and the cause of the damage.

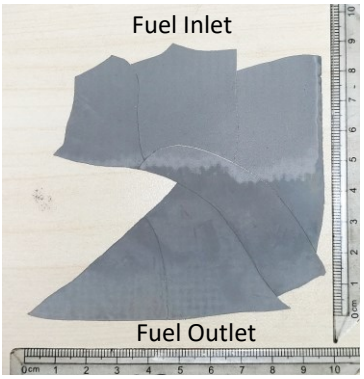

Fig 8 The anode of the upper cell after test

3.4 Conclusions and future work

The model successfully revealed the region where cell damage occurred using the measured temperatures and is potential to facilitate in-situ monitoring of stacks and early detection of stack problems.

Further efforts are required to calibrate the model for the other conditions in this test and to improve the heat source resolution so that the heat sources on the cells are distinguishable on different layers.

ACKNOWLEDGEMENT

This work was supported by Ministry of Science and Technology, China (MOST 2017YFB0601903).

REFERENCE

[1] Kirtley, J. D., Qadri, S. N., Steinhurst, D. A., & Owrutsky, J. C. In situ, simultaneous thermal imaging and infrared molecular emission studies of solid oxide fuel cell electrodes. J. Power Sources 2016;336:54–62.

[2] Li A, Lin Z. Efficient Mass Transport and Electrochemistry Coupling Scheme for Reliable Multiphysics Modeling of Planar Solid Oxide Fuel Cell Stack. Chinese Journal of Chemical Physics 2017;30(2):139-146.

[3] Nishida R T, Beale S B, Pharoah J G, et al. Three-dimensional computational fluid dynamics modelling and experimental validation of the Jülich Mark-F solid oxide fuel cell stack. Journal of Power Sources 2018; 373:203-210.

[4] GRI-Mech Version 3.0 Thermodynamics released 7/30/99, accessed on June.1st, 2019: http://combustion.berkeley.edu/gri_mech/version30/files30/thermo30.dat